Pergamon

Int. J. Mach. Tools Manufact. Vol. 37, No. 5, pp. 619–633, 1997

0890-6955/97$17.00 + .00

PII: S0890-6955(96)00055-7

APPLIED MECHANICS IN GRINDING—V. THERMAL RESIDUAL STRESSES

MOFID MAHDI† and LIANGCHI ZHANG†‡

(*Received* 15 *March* 1996)

Abstract—The objective of this part of the series research is to investigate the correlation between the thermal residual stresses and conditions of surface grinding. The heat generated in grinding was modelled by a moving band heat source with a triangular profile. The effect of a coolant was simulated by heat convection. To obtain a reliable figure of thermal residual stresses induced by grinding, temperature-dependent properties of work materials were taken into account and a non-uniform convection model with an effective cooling factor was introduced. A thorough analysis using the finite element method showed that the predictions based on the temperature-independent properties always underestimate thermal deformation, that the effective cooling factor in the grinding zone should be maintained beyond a critical value, and that the Peclet number has a significant effect on the selection of critical grinding conditions. The paper offers an insight into the mechanism understanding of thermal residual stresses induced by surface grinding.

NOMENCLATURE

a	thermal coefficient of expansion of work material
c	specific heat capacity per unit volume of workmaterial
D	elastic–plastic constitutive matrix
e	error
H	non-dimensional heat transfer coefficient ($2\alpha h/\kappa v$)
h	heat transfer coefficient of coolant
L_c	length of grinding zone, see Fig. 1
l_a	relative peak location of a heat flux ($2\zeta_a/L_c$), see Fig. 1
Pe	Peclet number ($vL_c/4\alpha$)
q	heat flux per unit grinding width
q_a	peak value of the heat flux
q_c	heat transferred by convection (hT), see Fig. 1
T	temperature rise with respect to ambient temperature T_∞
v	moving speed of the heat source, see Fig. 1
Y	yield stress of the work material
α	thermal diffusivity
ϵ	strain tensor
ζ, χ	coordinates, fixed to the moving heat source, see Fig. 1
κ	thermal conductivity of work material
ν	Poisson's ratio
σ	stress tensor
ω	effective cooling factor within the grinding zone, defined by Equation (2)
Subscripts	
m	mechanical
T	thermal
x, y, z	x-, y- and z-directions
Y	yield
1, 2, 3	maximum, intermediate and minimum principal directions
∞	room temperature

1. INTRODUCTION

Thermal plastic deformation induced by the heat generated in grinding is one of the major causes of residual stresses of grinding. Therefore to evaluate adequately thermal residual stresses in a ground component, the strength and distribution of the heat source, the con-

†Department of Mechanical and Mechatronic Engineering, The University of Sydney, Sydney, NSW 2006, Australia.

‡Author to whom correspondence should be addressed.

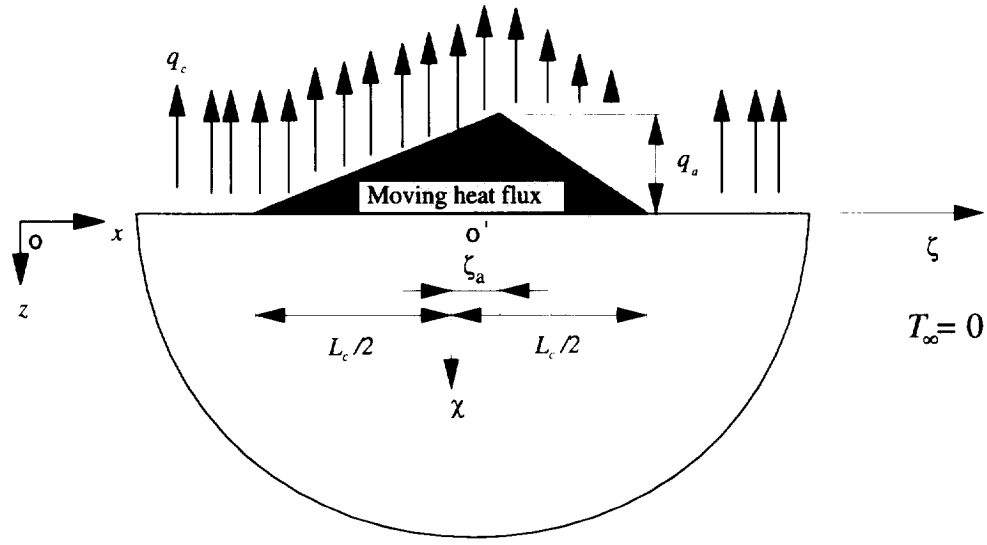

Fig. 1. A theoretical model of surface grinding with non-uniform convection.

vection mechanisms of cooling media and the thermal properties of the work material need to be carefully taken into account.

Previous studies on residual stresses associated with grinding considered that the grinding heat source had a constant strength over the grinding zone (e.g. Refs [1, 2]). However, in Refs [3–6] it was shown that the strength of the heat source in a theoretical modelling should vary in the grinding zone and could be properly described by a triangular profile with an adjustable apex to accommodate the effect of different grinding operations. Nevertheless, it was assumed in Refs [5, 6] that the convection heat transfer coefficient of coolant was uniform over the whole workpiece surface. This is not very consistent with a real grinding operation, because inside a grinding zone there is usually much less coolant, and the coolant there may evaporate. Thus the convection rate inside is generally lower. In addition, because of the non-uniform convection over a workpiece surface, temperature-dependent properties of the work material may play a more important role.

This paper aims to investigate the thermal residual stresses induced by grinding using a non-uniform convection model. To generate a reliable figure, the properties of work materials are considered to be temperature-dependent.

2. ANALYSIS

2.1. *Convection model*

For simplicity, the surface grinding process is assumed to be two-dimensional so that plane-strain conditions apply [1–6]. The heat source profile is triangular, moving along the positive direction of the x-axis on the workpiece surface, as shown in Fig. 1. To simulate a real convection heat transfer mechanism of grinding, a convection model must be able to reflect the different cooling rates inside and outside the grinding zone. To do this, we introduce the following analytical model of non-uniform convection that accounts for a partial cooling in the grinding zone:

$$q_c = \begin{cases} h_i T, & |\zeta| \le \dfrac{L_c}{2} \\ hT, & |\zeta| > \dfrac{L_c}{2} \end{cases} \tag{1}$$

where q_c is the heat transfer due to convection, T is the temperature rise induced by grinding, h and h_i are the convection heat transfer coefficients outside and inside the grinding zone, ζ is the local horizontal coordinate attached to the moving heat source, and

L_c is the grinding zone length. Generally speaking, h_i is a function of temperature, speed of grinding wheel, interfacial stresses in the grinding zone and the method of coolant application. For simplicity, we first assume that $h_i=\omega h$, where $\omega\leq 1$ is a positive constant factor and is called the effective cooling factor in the grinding zone. In so doing, Equation (1) is simplified to

$$q_c=\begin{cases}\omega hT, & |\zeta|\leq \dfrac{L_c}{2}\\ hT, & |\zeta|>\dfrac{L_c}{2}\end{cases} \tag{2}$$

Obviously, the value of ω for a specific grinding operation depends strongly on the cooling efficiency within the grinding zone, or in other words, relies on the soundness of the method of coolant application. When $\omega=1$, the convection becomes uniform over the whole workpiece surface.

2.2. *Constitutive equation*

To predict the thermal stresses, an incremental constitutive relationship between incremental stresses and strains must be used. Such a relationship can be written as [7]

$$\Delta\sigma=\mathbf{D}(\Delta\epsilon_m-\Delta\epsilon_T), \tag{3}$$

where $\Delta\sigma$ is the incremental stress vector, $\mathbf{D}$ is the elastic–plastic constitutive matrix, $\Delta\epsilon_m$ is the incremental mechanical strain vector, and $\Delta\epsilon_T$ is the incremental thermal strain vector determined by

$$\Delta\epsilon_T=\begin{Bmatrix}\Delta\epsilon_{Tx}\\ \Delta\epsilon_{Tz}\\ \Delta\epsilon_{Ty}\end{Bmatrix}=(1+\nu)\begin{Bmatrix}a\Delta T\\ a\Delta T\\ 0\end{Bmatrix} \tag{4}$$

In Equation (4), $\Delta\epsilon_{Tx}$, $\Delta\epsilon_{Ty}$ and $\Delta\epsilon_{Tz}$ are, respectively, the incremental thermal strains in the x-, y- and z-directions, ν is Poisson's ratio, ΔT is the temperature rise increment and a is the thermal coefficient of expansion. It should be noted that Equation (3) is strongly non-linear and needs to be integrated numerically. This will be carried out by the finite element method.

2.3. *Control volume and its meshing*

Assume that the dimensions of the workpiece under surface grinding are much greater than the length of grinding zone. Hence the control volume in the finite element analysis must be sufficiently large, and the number and size of elements appropriate to generate reliable residual stresses because a moving heat source is involved. In addition, a remeshing technique must be used to guarantee the reliability of the numerical results; that is, mesh refinement continues until the effect of any further remeshing on the final result becomes negligible. In this study the control volume and finite element division are considered to be reliable when a stable error of less than 4% is achieved in further variations of the mesh configurations and dimensions of control volumes. After a series of trial calculations, the control volume of $16L_c\times 6L_c$ with 1536 nine-noded elements and 6321 nodes, as shown in Fig. 2, was found to be the most appropriate in terms of the computational efficiency, numerical stability and simulation accuracy. Such a control volume selection and domain division guarantee that the accumulated computational error in temperature prediction is within 3.5%, which is acceptable to most engineering applications. A typical error analysis is shown in Fig. 3.

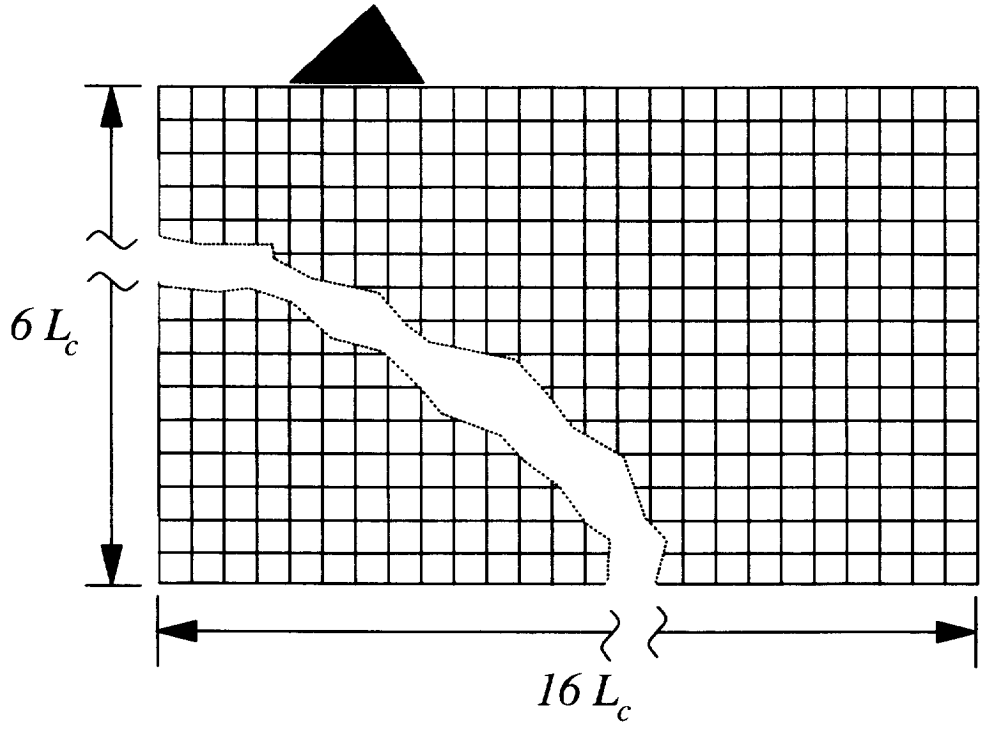

Fig. 2. Finite element division of the control volume.

2.4. *Temperature-dependent properties*

In principle, material properties such as Young's modulus, Poisson's ratio, yield stress, thermal heat conductivity, specific heat capacity, thermal expansion coefficient and so on are all temperature dependent. However, in a certain temperature range, the variation of some properties is negligible compared with the others. When grinding with effective cooling, the most sensitive temperature-dependent variables for a large class of typical engineering alloys are thermal conductivity κ and specific heat capacity c. This is true for the alloy steel EN23 [8] to be investigated in the present study. In the following analysis, therefore, we will only consider the variation of κ and c of EN23 whenever the temperature-dependent properties are concerned. The properties of EN23 are shown in Table 1 and Fig. 4. It is clear that the dependence of κ and c upon temperature rise is complex and makes the thermal deformation of the material strongly non-linear.

3. RESULTS AND DISCUSSION

3.1. *Effects of material properties and cooling mechanisms*

For the convenience of discussion, let us define the critical grinding condition as that causing the onset of plastic deformation under thermal loading. When other grinding parameters, such as the Peclet number Pe, apex of input heat flux l_a, and effective cooling factor ω, are given, the critical grinding condition is represented by the peak value of the input heat flux q_a that is the resultant of the wheel depth of cut and material removal mechanism in a specific grinding process.

Figure 5 shows the effect of material properties on the critical grinding condition. The workpiece is purely elastic when a grinding state is below a critical curve, but becomes elastic–plastic when it is above the curve. The figure demonstrates that the predictions based on the temperature-independent calculations always overestimate the critical level of input heat flux corresponding to the onset of yielding of the work material. In other words, thermal plastic deformation may have occurred in the work material when the prediction still indicates a purely elastic state. This becomes more severe when Pe is large. It is understandable if the real material properties shown in Fig. 4 are recalled. A temperature-independent analysis uses the mean values of κ and c, and the critical temperature

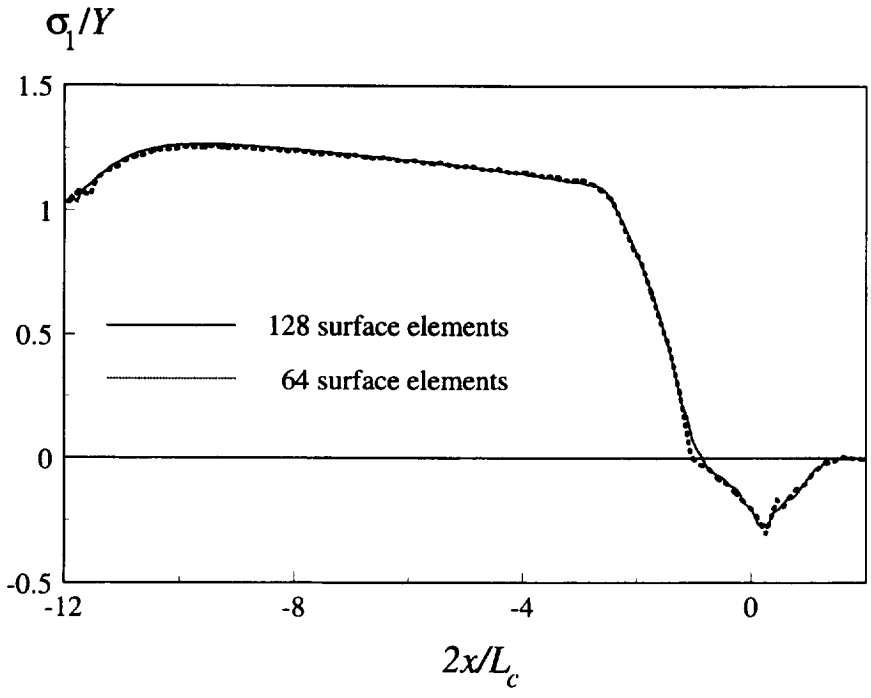

(a)

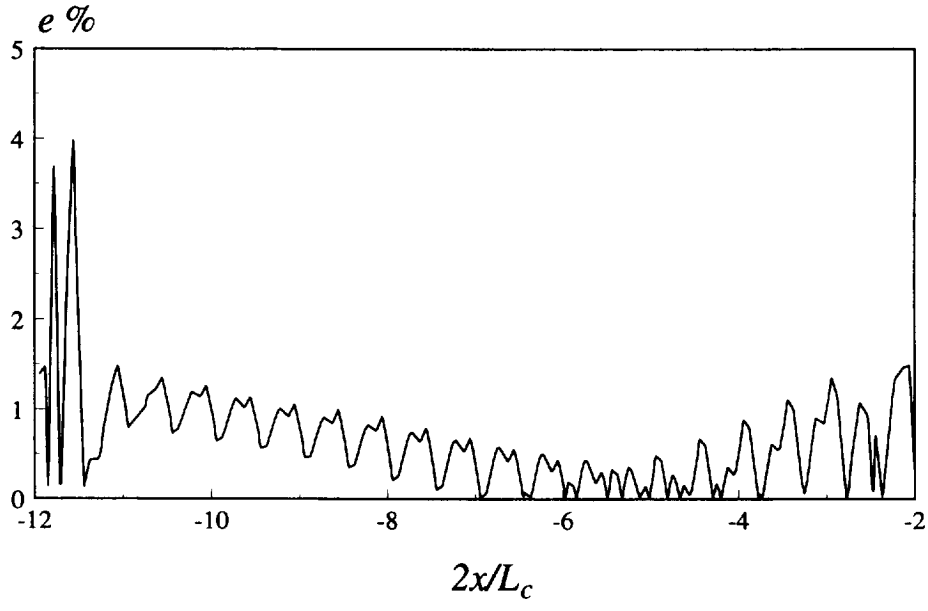

(b)

Fig. 3. Mesh refining effect (H_∞=0.0, l_a=0.25, Pe_∞=1 and q_a=80 MW/m^2): (a) surface stress; (b) relative error.

Table 1. The composition and mechanical properties of alloy steel EN23

Composition (wt%)						Yield stress (MPa)	Young's modulus (GPa)	Thermal coefficient of expansion (C^{-1})	Poisson's ratio
C	Si	Mn	Cr	Mo	Ni				
0.3	0.25	0.55	0.71	0.06	3.41	796	214	1.4×10^{-5}	0.27

for the initiation of thermal plastic deformation in EN23 is around 300°C. When $T\leq500$°C, the real c is very close to its average. Nevertheless, the real κ of the material in this temperature regime is much higher than its mean value. This implies, if compared with the prediction of the temperature-independent model, that much more heat actually flows into the workpiece subsurface and that the locally induced thermal deformation is much greater. Figure 5 also shows that the effect of l_a is not significant. Thus the thermal plastic deformation generated by an up- or a down-grinding operation will not be very different.

Figure 6 examines the effect of cooling mechanisms on the critical grinding condition. Clearly, any cooling mechanisms associated with grinding fall in the band limited by the curve with $\omega=0$, indicating no cooling within the grinding zone, and that with $\omega=1$, representing a uniform cooling over the whole workpiece surface [see Fig. 6(a)]. When Pe is larger, the cooling band is wider, denoting that the effective cooling in the grinding zone becomes more important when the table speed of grinding becomes higher. Figure 6(b) demonstrates the effects of l_a and ω with a given Pe. It shows once again the importance of effective cooling in the grinding zone. The apex of the input heat flux also has an effect on the critical grinding condition. $l_a=0.25$ is the most critical heat input profile. It is worth noting that the difference of the critical q_a of initiating thermal plastic deformation between the cases of $l_a=0.25$ and 1.0 is considerable even under the condition of uniform convection ($\omega=1$).

3.2. *Mechanisms of residual stress formation*

The heat generated within the grinding zone causes a very non-uniform temperature field in the workpiece and in turn causes considerable localized thermal deformation. Thus a complex stress field is created by the internal restrains of material constituents and the boundary conditions imposed. As the heat source moves along the workpiece surface, the associated temperature field and thermal deformation also vary (see Figs 7 and 8). Clearly, the transient temperature field and thermal deformation approach their quasi-steady states after a few movement steps of the heat flux.

The part of the work material subjected to a higher temperature rise expands more significantly and causes compressive stresses because of the restraint from its surrounding material that expands less. When the stress field exceeds the yield limit of the material, plastic deformation due to the non-uniform thermal expansion takes place. A plastic zone of thermal loading is then developed [Fig. 8(a)]. Nevertheless, when the surface heat source moves forward, the material outside the grinding zone contracts under a more effective coolant application. Since a part of the work material has been plastically deformed during thermal loading, the contraction is greatly restrained and thus a tensile stress field is generated locally. Furthermore, when the tensile stress level is sufficiently high, a reverse yielding occurs and a plastic zone of thermal unloading appears [Fig. 8(b)]. Therefore, a complex residual stress field in the ground work material is produced. That is why the surface thermal residual stresses in a ground component are usually tensile. The above process of development of plastic zones is clearly shown in Fig. 8.

From the point of view of mechanics, the thermal residual stress field in a ground component is the final stable state of transient thermal stresses. Therefore a thorough examination of the transient process of the thermal stress development would help understand the relationship between grinding conditions and residual stress distributions. Figure 9 reveals the correlation between the surface temperature change and variation of

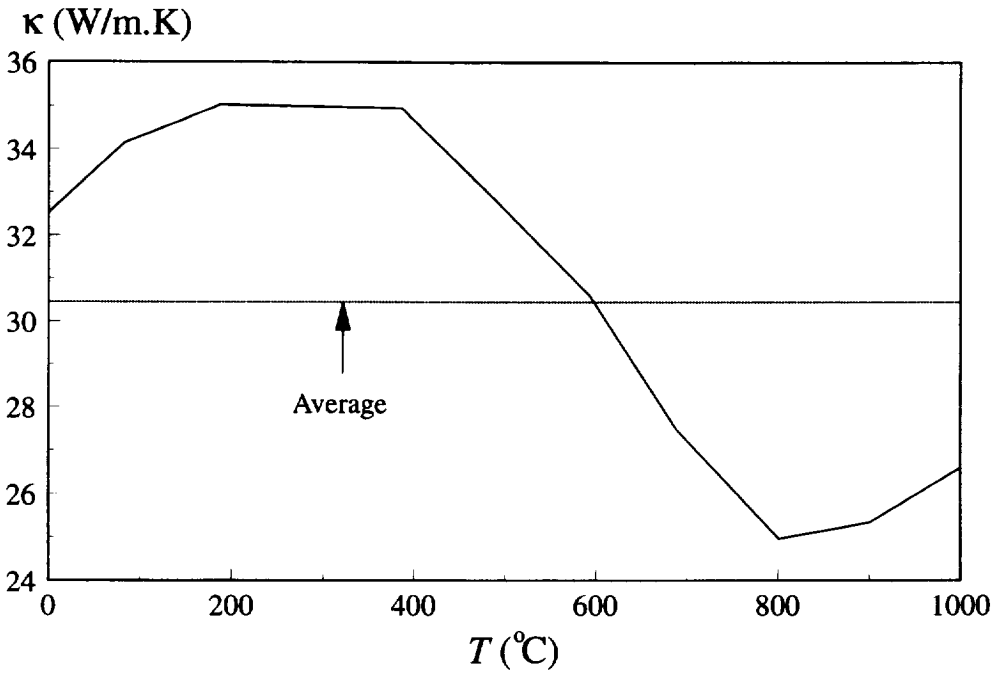

(a)

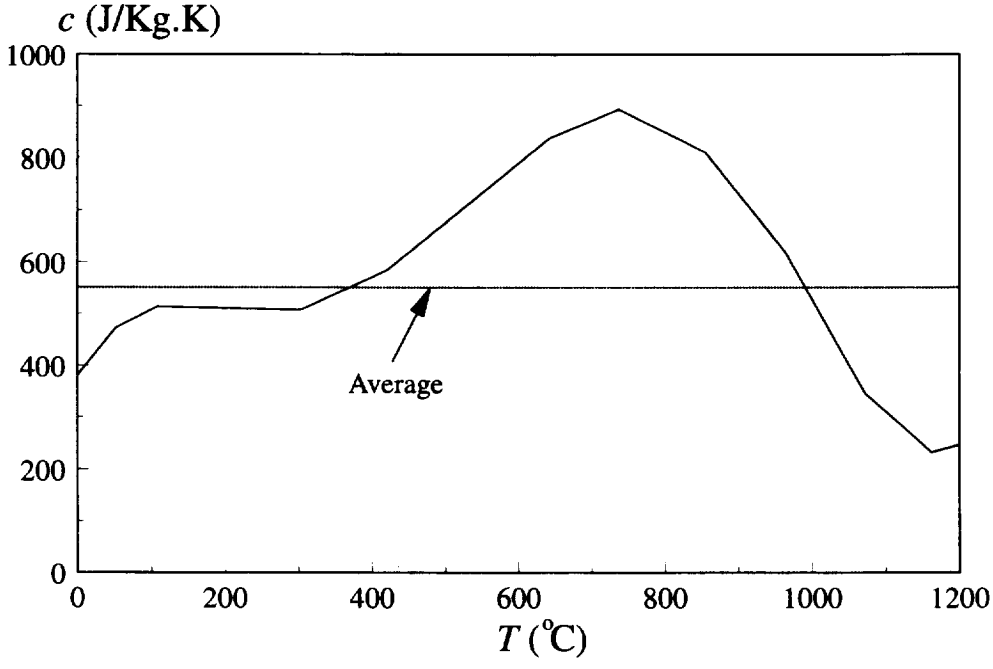

(b)

Fig. 4. Thermal properties of alloy steel EN23: (a) thermal conductivity; (b) specific heat capacity

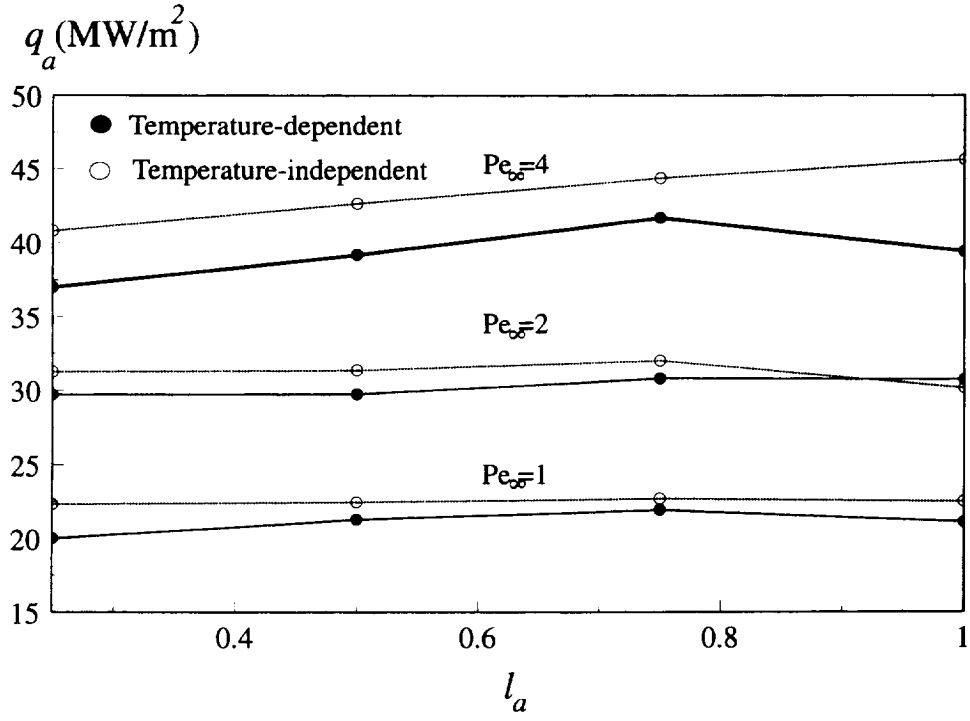

Fig. 5. Critical grinding conditions versus temperature-dependent properties (H_{∞}=0.0).

maximum surface residual stress, σ_1. The figure shows that the compressive surface stress only appears within the grinding zone during the transient process. The peak of this compressive stress is coincident with the maximum surface temperature rise. σ_1 becomes highly tensile almost immediately outside the grinding zone. When the heat flux moves forward, the distribution of the surface stress far away from the grinding zone (>5L_c, for example) becomes stable and forms the surface residual stress.

The apex of the input heat flux l_a influences the onset of thermal plastic deformation in the work material, as discussed above, and thus affects the final residual stress field. Figure 10 shows that l_a largely alters the distribution of σ_1 near the end of the workpiece where grinding starts. In all the other parts of the workpiece, the effect of l_a is not as big as that of the Peclet number Pe (Fig. 11). Hence the variation of the thermal residual stresses induced by l_a can be ignored if the prediction accuracy needs not be very high, particularly in the cases with high q_a values. However, surface residual stresses are very dependent on the Peclet number. For a given strength of the heat input q_a, a lower Pe produces higher surface residual stresses and vice versa (Fig. 11).

The effective cooling factor ω is a key factor in determining the maximum surface residual stress and thickness of the surface layer subjected to tensile stress (see Figs 12 and 13). This becomes more dominant at a high convection heat transfer. It is interesting to note (Fig. 12) that if ω is small, larger convection heat transfer coefficients (H_{∞}) may not bring about lower levels of residual stresses. Only when $\omega \geq 0.66$ does the increase of H_{∞} always result in lower residual stresses, which is more desirable in a practical application. Furthermore, although the increase of H_{∞} has an overall effect in reducing the magnitude of surface tensile stress when $\omega \geq 0.66$, it does not change the thickness, t, of the surface layer under a large tensile stress (Fig. 13). The thickness alteration can be achieved by changing ω. In the present study with the alloy steel EN23, the layer thickness can be reduced from t=0.5 to 0.4 when ω varies from 0 to 1. All of the above results strongly suggest that a coolant application method should aim to obtain an effective cooling factor larger than 0.66 while using a coolant with a high H_{∞}. However, although the critical value of ω for EN23 is 0.66, it may differ from material to material.

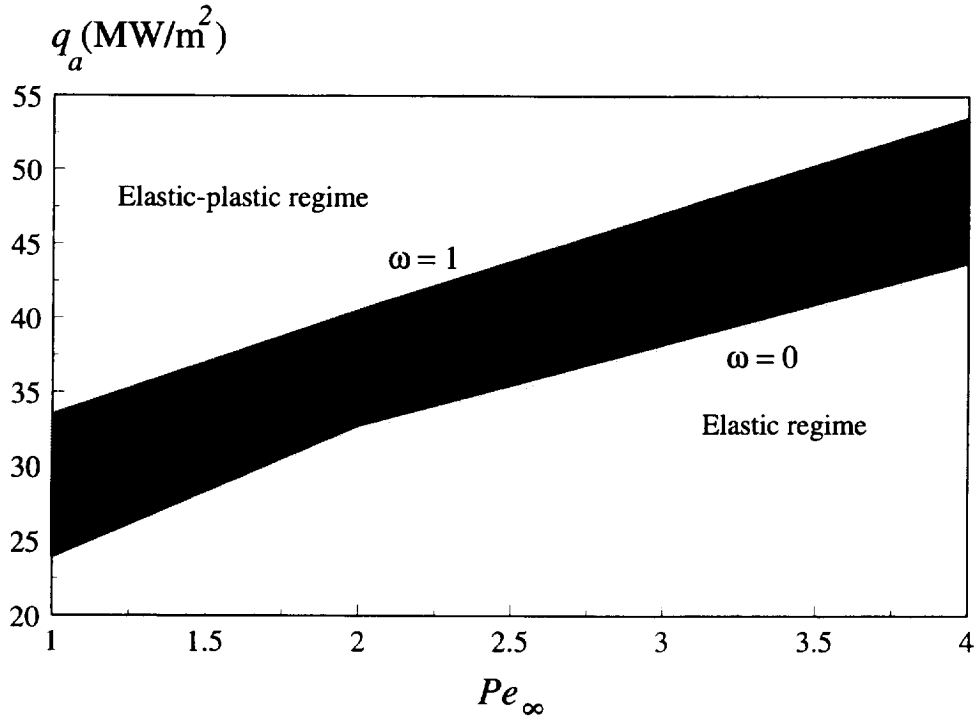

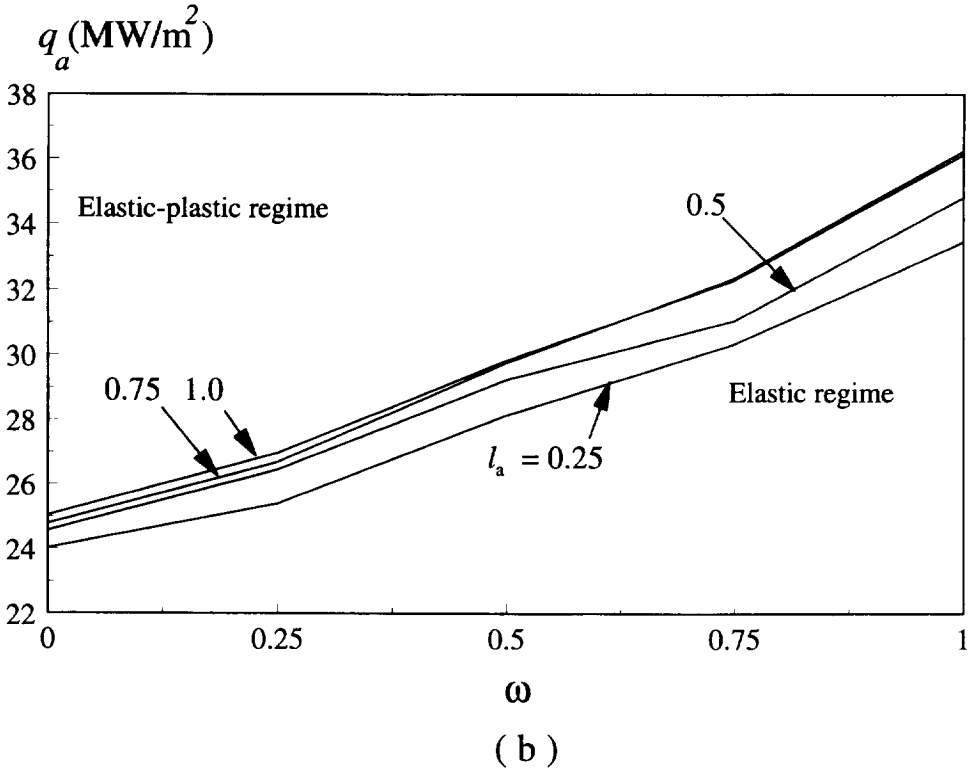

Fig. 6. Critical grinding conditions versus cooling mechanisms (H_∞=1.0): (a) l_a=0.25; (b)Pe_∞=1.

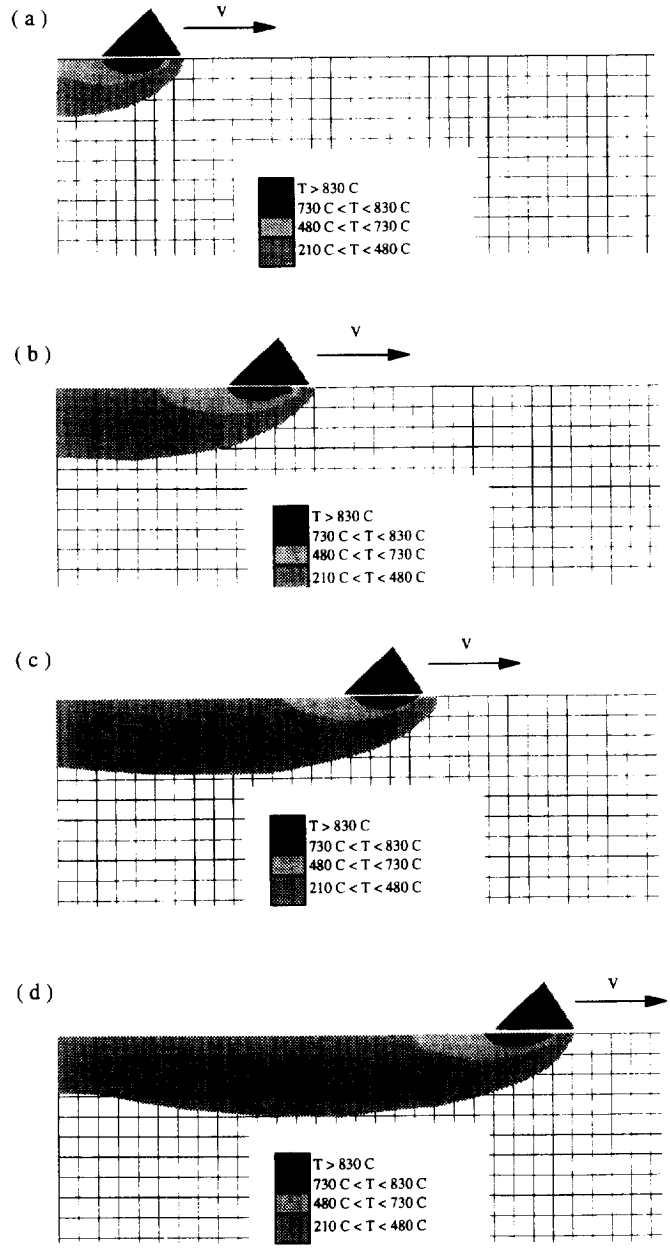

Fig. 7. The variation of temperature field with heat source movement. The instant coordinate of the heat source centre is $X_{centre}=2x/L_c$. ($\omega=1.0$, $H_z=0.0$, $l_a=0.25$, $Pe_z=1$ and $q_a=85$ MW/m^2): (a) $X_{centre}=2.25$; (b) $X_{centre}=5.25$; (c) $X_{centre}=9.25$; (d) $X_{centre}=12.00$.

4. CONCLUSIONS

A thorough analysis of the thermal residual stresses induced by surface grinding has been conducted with the aid of the finite element method. A non-uniform convection model has been proposed to simulate a real cooling process. The effect of temperature-dependent properties of work materials has been carefully examined. The study concludes the following:

(1) Predictions based on the temperature-independent properties always underestimate the onset of thermal plastic deformation; thus temperature-dependent effects must be taken into account if an accurate prediction of thermal residual stresses is expected.
(2) A high cooling rate is more advantageous in minimizing the thermal residual stresses, if the effective cooling factor in the grinding zone can be maintained above a critical value.

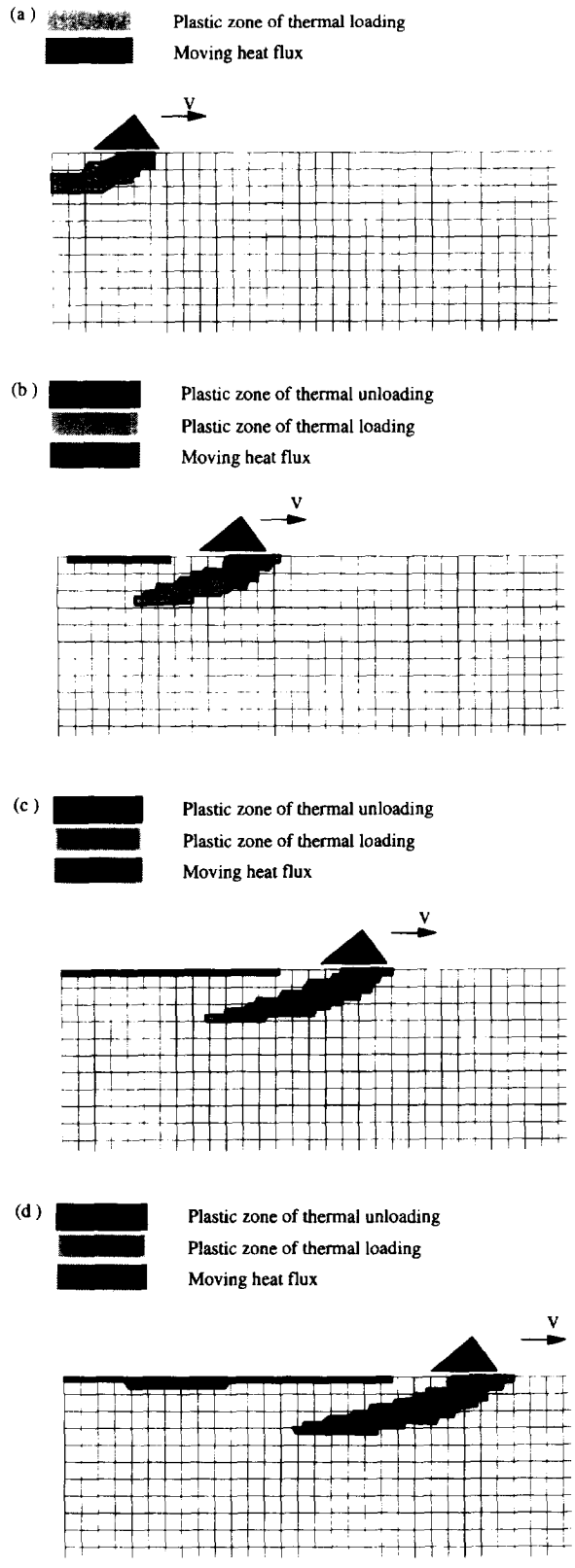

Fig. 8. Development of plastic zones during grinding (ω=1.0, H_∞=0.0, l_a=0.25, Pe_∞=1 and q_a=85 MW/m^2): (a) X_{centre}=2.25; (b) X_{centre}=5.25; (c) X_{centre}=9.25; (d) X_{centre}=12.00.

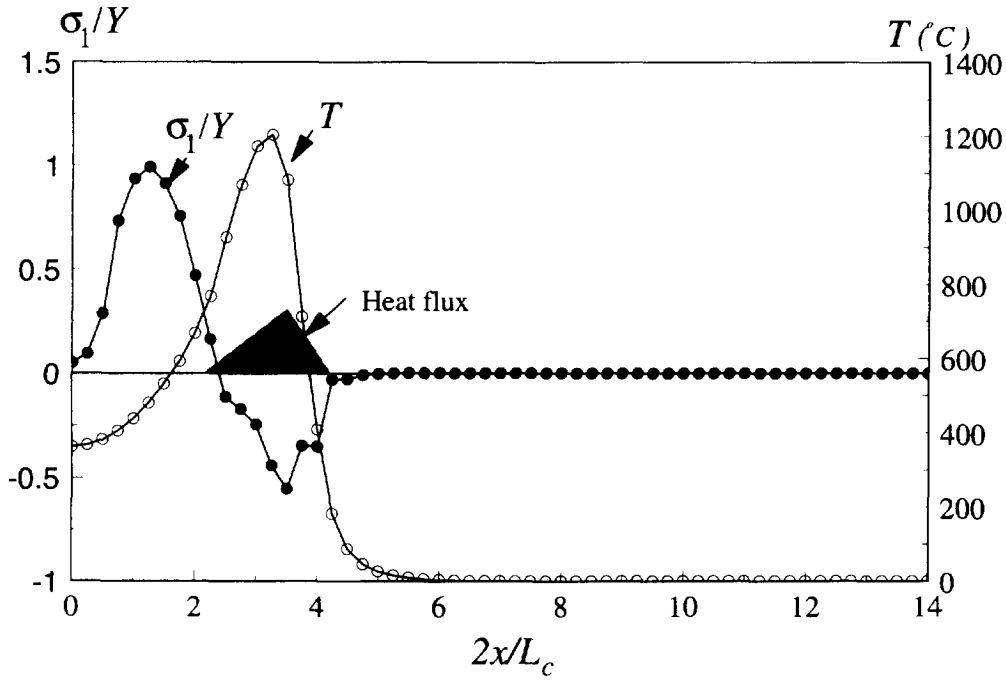

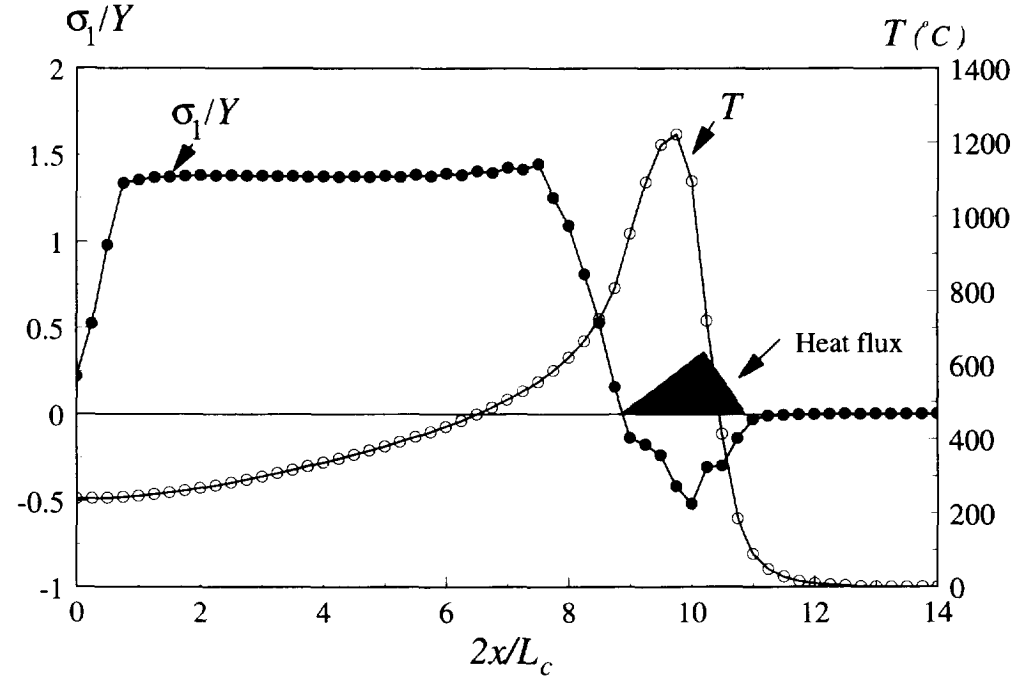

Fig. 9. Surface thermal grinding stresses versus temperature history (q_a=85 MW/m^2, H_∞=0.0, l_a=0.25 and Pe_∞=1).

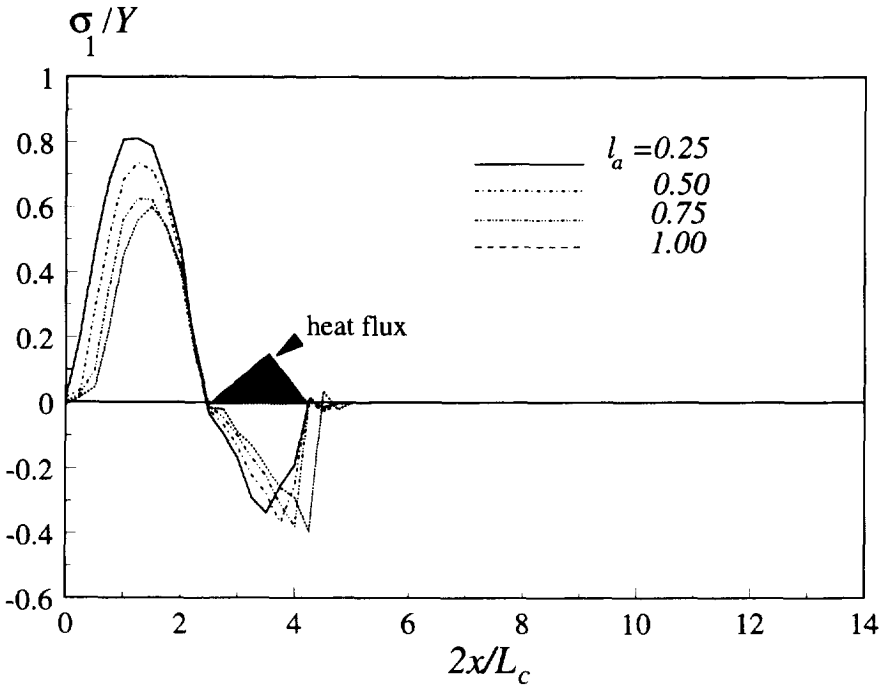

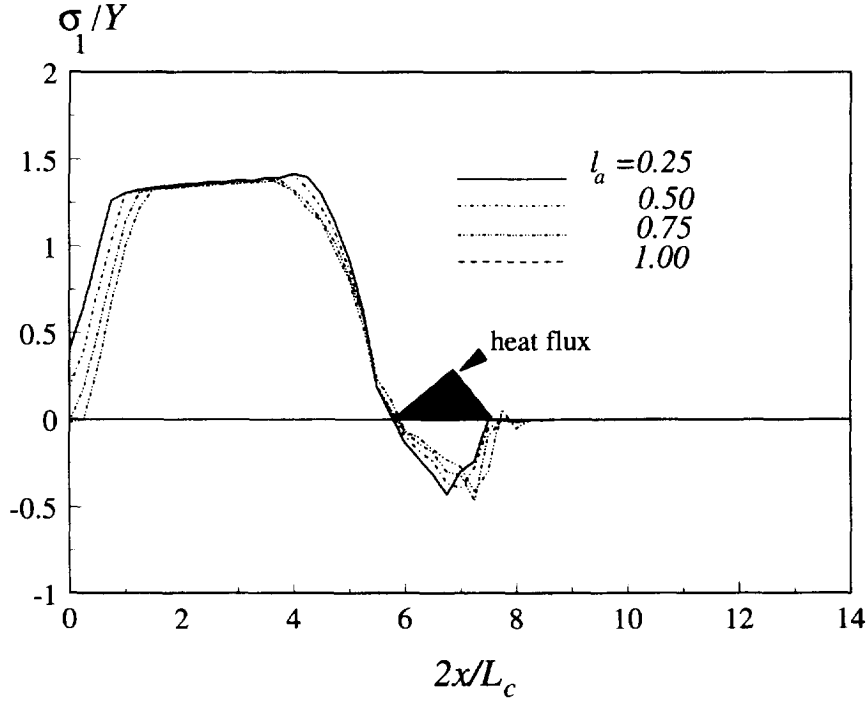

Fig. 10. Effect of l_a on the surface stress development (q_a=85 MW/m^2, Pe_∞=1, H_∞=1.0 and ω=1.0).

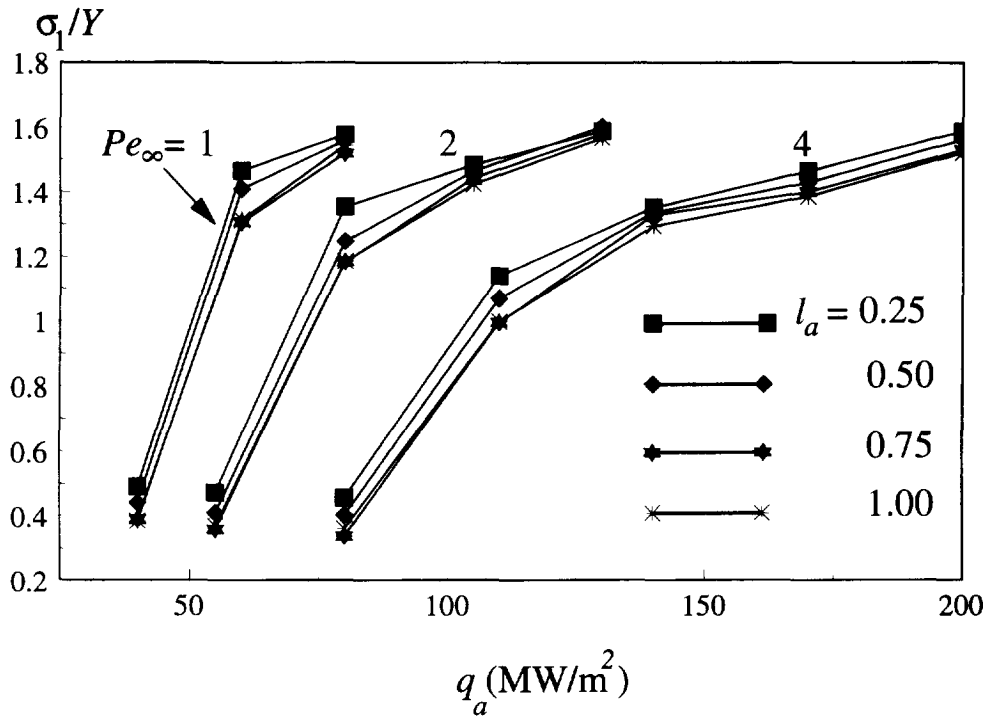

Fig. 11. Effect of Pe_∞ on the maximum surface residual stress (H_∞=0.0 and l_a=0.25).

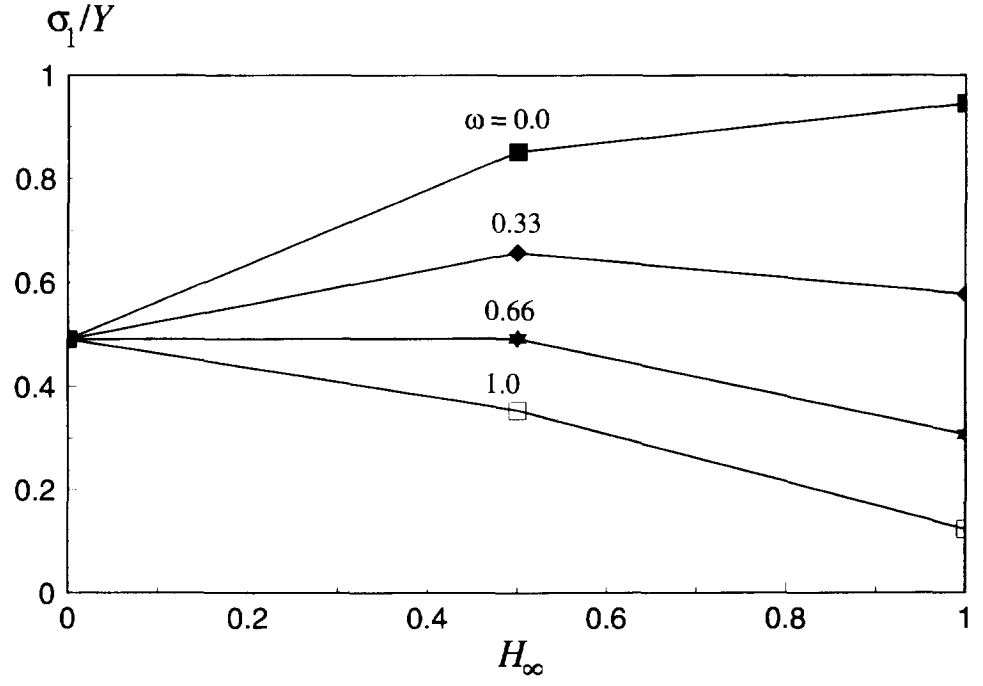

Fig. 12. Variation of surface thermal residual stresses with the effective cooling factor in grinding zone (Pe_∞=1 and q_a=40 MW/m^2).

(3) The Peclet number of a grinding operation affects the critical grinding condition more significantly than the details of the input heat flux profile.

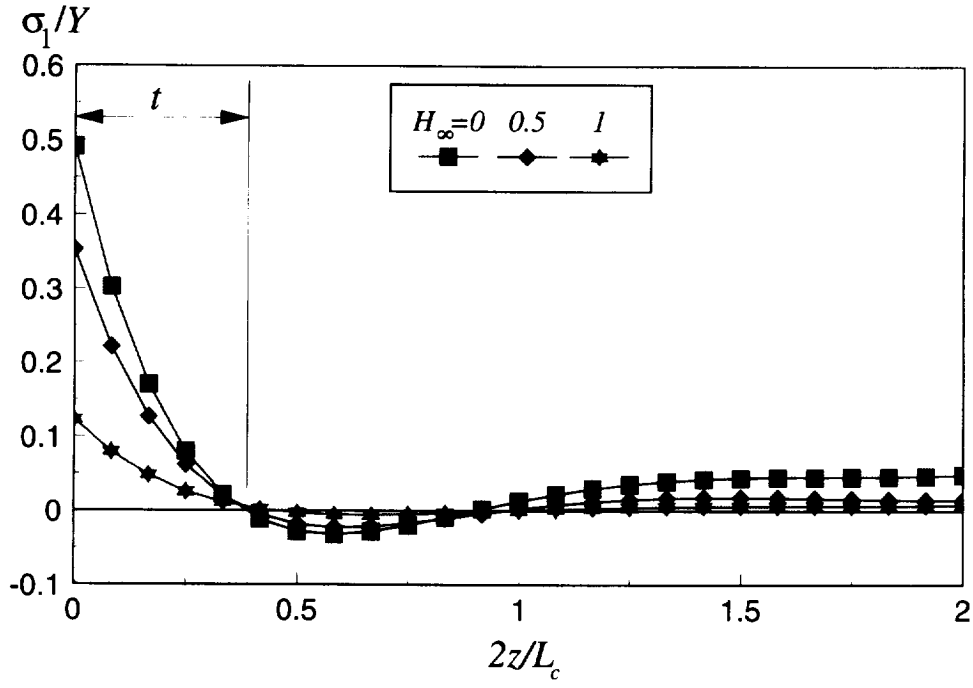

Fig. 13. Distribution of thermal residual stresses in the depth direction (q_a=40 MW/m^2, Pe_x=1, H_x=1.0 and ω=1.0).

Acknowledgements—The financial support to the present study from the ARC Small Grant is very much appreciated. ADINA code was used for all the calculations.

REFERENCES

[1] Y.Y. Li and Y. Chen, Simulation of surface grinding, *J. engng Mater. Technol. Trans. ASME* **111**, 46–53 (1989).
[2] A. Mishra and T. Prasad, Residual stresses due to a moving heat source, *Int. J. mech. Sci.* **27**, 571–581 (1985).
[3] L. C. Zhang, T. Suto, H. Noguchi and T. Waida, On some fundamental problems in grinding. In *Computer Methods and Experimental Measurements for Surface Treatment Effects* (edited by M. H. Aliabadi and C. A. Brebbia), pp. 275–284. Computational Mechanics Publications, Southampton (1993).
[4] L.C. Zliang, T. Suto, H. Noguchi and T. Waida, An overview of applied mechanics in grinding, *Manufact. Rev.* **5**, 261–273 (1992).
[5] L.C. Zliang and M. Mahdi, Applied mechanics in grinding, part IV: grinding induced phase transformation, *Int. J. Mach. Tools Manufact.* **35**, 1397–1409 (1995).
[6] M. Mahdi and L.C. Zhang, The finite element thermal analysis of grinding processes by ADINA, *Comput. Struct.* **56**, 313–320 (1995).
[7] ADINA R&D Inc, Version 6.1 (1992).
[8] British Iron and Steel Research Association, *The Mechanical and Physical Properties of the British Standard on Steels*, Vol. 2. Pergamon, Oxford (1969).